University of Sistan and Baluchestan

Challenges in Nano and Micro Scale Science and Technology

Online ISSN: 2821 - 000X

A Study on The Adsorption of Methylene Blue on Polydopamine@Zeolitic Imidazolate-67 in Aqueous Solution

Maryam Hajnajafi[1] | Alireza Khorshidi[2]✉ | Ali Ghanadzadeh Gilani[3] Francis Verpoort[4]

1. Department of Chemistry, Faculty of Sciences, University of Guilan, P. O. Box: 41335-1914, Rasht, Iran
2. Corresponding Author, Department of Chemistry, Faculty of Sciences, University of Guilan, P. O. Box: 41335-1914, Rasht, Iran. Email: khorshidi@guilan.ac.ir
3. Department of Chemistry, Faculty of Sciences, University of Guilan, P. O. Box: 41335-1914, Rasht, Iran
4. National Research Tomsk Polytechnic University, Lenina Ave. 30, Tomsk 634050 Russia
   Laboratory of Organometallics, Catalysis and Ordered Materials, State Key Laboratory of Advanced Technology for Materials Synthesis and Processing, Wuhan University of Technology, Wuhan, PR China
   Ghent University, Global Campus Songdo, 119 Songdomunhwa-Ro, Yeonsu-Gu, Incheon 406-840, South Korea

Article Info

Article type:
Research Article

Keywords:
Adsorption,
ZIF-67,
Polydopamine,
Thermodynamics,
Kinetics.

ABSTRACT

Polymer-modified metal organic frameworks (MOFs) can enhance water purification processes by offering increased adsorption capacity, making them highly effective in separating pollutants from contaminated water. In this research, a facile and low-cost route was used to prepare Polydopamine@Zeolitic Imidazolate Framework-67 (PDA@ZIF-67). The structure, morphology, surface functional groups and particle size distribution of PDA@ZIF-67 was studied using Fourier-transform infrared spectroscopy (FTIR), Field emission scanning electron microscopy (FESEM), Energy dispersive spectroscopy (EDS), and Brunauer-Emmet-Teller (BET) analyses. The specific surface area and pore diameter of PDA@ZIF-67 nanoparticles were found to be 203.78 m^2/g and 4.179 nm, respectively. The PDA@ZIF-67 was used as an adsorbent for removal of methylene blue dye from aqueous solution. The results showed that the maximum adsorption capacity of PDA@ZIF-67 for removal of MB was achieved at pH 2, 65 °C, 10 mg of adsorbent, and methylene blue concentration of 7.5 ppm. Moreover, the adsorption process isotherms, thermodynamics, and kinetics were studied to ascertain the adsorption mechanism. The methylene blue molecules located in the fine pores of the PDA@ZIF-67 adsorbent determine the adsorption rate. Moreover, it was found that the adsorption process of methylene blue at elevated temperature is a spontaneous and endothermic reaction. The adsorption capacity of PDA@ZIF-67, after six recovery cycles decreased to 62.21%, which can be considered as an excellent advantage for this adsorbent.

INTRODUCTION

Rapid growth of chemical industries along with the expansion of agriculture has led to severe pollution of water resources [1]. This topic is considered as a global problem [2]. Among the various types of water pollutants, dyes have been emerged as one of the most important issues in the scientific community [3].

Methylene blue (MB) with the molecular formula of $C_{16}H_{18}ClN_3S$ (Figure 1) is an organic cationic dye, which has been widely used in biological and chemical applications. Large amounts of organic dye effluents are produced annually by related industries such as printing, textiles, dyeing, papermaking, etc. Colored effluents have undesirable properties such as high biological oxygen demand (BOD), poor biodegradation, toxic nature, and so on. These properties are dangerous to living organisms including photosynthesizing ones [4].

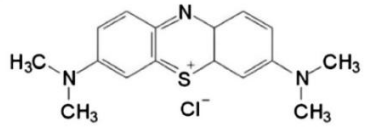


Fig. 1. Chemical structure of methylene blue

How to Cite this paper: Hajnajafi M, Khorshidi A, Ghanadzadeh Gilani A, Verpoort F. A Study on The Adsorption of Methylene Blue on Polydopamine@Zeolitic Imidazolate-67 in Aqueous Solution. *Challenges in Nano and Micro Scale Science and Technology*. 2023; 11(1): 1-10. DOI: 10.22111/cnmst.2024.48237.1246

© Hajnajafi M, Khorshidi A, Ghanadzadeh Gilani A, Verpoort F. Publisher: University of Sistan and Baluchestan.
DOI: 10.22111/cnmst.2024.48237.1246

such as advanced oxidation processes (AOP) [5], membrane filtration [6], flocculation [7], ozonation [8], photocatalytic degradation [9], biodegradation [10], membrane technology [11] and coagulation [12] have been used to remove organic pollutants from aqueous phase. However, application of traditional methods still faces two inherent limitations including complexity and economic inefficiency. Therefore, finding an easy, economical and effective method for wastewater treatment has emerged as a hot topic in scientific community. Adsorption on the surface of a suitable adsorbent is another common method for removal of contaminants. Carbon materials [13], minerals (including kaolinite and montmorillonite) [14], polymers [15], zeolites [16], clays [17], sludge [18], flax fibers [19], and biochar [20], are some of the most widely used adsorbents in this regard.

Nevertheless, poor performance of the conventional adsorbents in terms of selectivity and capacity has been emerged as a fundamental problem. Designing hybrid materials for the adsorption of dyes is aimed at addressing the environmental impact of industrial wastewater, particularly from the textile industry. These hybrid materials are engineered to combine multiple functionalities into a single treatment solution, enhancing efficiency and stability. For instance, the integration of green polymer conductive adsorbents with metal oxides and conductive polymers has shown promising results in removing dyes like pink-XFG from wastewater. The synthesis of such materials often involves advanced techniques like precipitation copolymerization, ensuring their thermal stability and reusability. By optimizing the adsorption process in both batch and column modes, these hybrid materials can achieve high adsorption capacities, with some materials showing potential for many cycles of use. In recent years, metal-organic frameworks (MOFs), due to their high porosity and surface area, large adsorption capacity, and desirable guest-host interactions, have been employed as a promising alternative in various applications including drug delivery and adsorption processes. High adsorption capacity of MOFs has been attributed to the electrostatic interactions, conjugated π-π interactions, and hydrogen bonds. Since the MOFs show good thermal and chemical stability, they have been used in various fields such as gas adsorption, molecular separation and electrochemistry. One of the most studied metal organic frameworks is Zeolitic Imidazolate-67 (ZIF-67), which consists of Co^{2+} ions linked by 2-methylimidazolate linkers to form a cubic crystal structure with the unit cell parameters of a = b = c = 16.9585 Å**.** Zeolitic Imidazolate-67 offers a three-dimensional (3D) structure with a high tendency to adsorb contaminants in the aqueous media. However, the application of ZIF-67 as an adsorbent still faces three vital problems including low specific surface area, poor structural stability, and difficult separation**.** Polydopamine (PDA) is one of the dopamine derivatives [21]. The unique properties of PDA (size control, uniform spherical shape, thermal stability, good biocompatibility and non-toxicity) have led to its application in various fields [22]. Moreover, the presence of NH and catechol groups in PDA leads to the application of this compound as an active adsorbent. Recently, scientists have proven that some polymers can be utilized as effective adsorbents for removal of pollutants. A porous magnetic carboxylic polymer as an efficient adsorbent for wastewater treatment was reported by Huang et al [23]. Zhang and co-workers modified a cationic magnetic chitosan grain polymer for efficient adsorption of heavy metals and dyes in a wide range of pH [24]. In recent years, scientists have found that the polymer-doped ZIF-67 can be utilized to overcome the above-mentioned challenges. Owing to the -OH functionality and its hydrophilic nature, PDA can be easily used as a dopant for ZIF-67, to provide a readily dispersible composite material. It has been shown that the porous structure of the PDA does not block the ZIF-67 holes [25]. In this work, we have tried to identify the shortcomings, and the existing gaps of the previous research as the main goal. Although the prior studies have had valuable results [26-29], our research was aimed to improve their achievements. By doing so, we aim to provide a more robust framework that can serve as a foundation for future research, thereby bridging the gaps identified in earlier studies and pushing the boundaries of our understanding further.

As mentioned above, polymer-extended porous materials, including MOFs, have emerged as novel solutions for removal of contaminants from aqueous solutions. In this contribution, preparation and application of a new hybrid material consisting of ZIF-67 and PDA is reported. The PDA@ZIF-67 was used as an efficient adsorbent for removal of MB dye from aqueous solution. Effect of various parameters on the adsorption of MB, including the reaction time, initial dye concentration, absorbent dosage, pH, temperature, and PDA: ZIF-67 ratio was studied, as well as the kinetics and thermodynamics of the adsorption process. The novel features of the present research may include, but not limited to, hybridization of ZIF-67 as a representative MOF with polydopamine, ease of polymer extension on the ZIF-67 support, high adsorption capacity, and in-depth study of kinetics and thermodynamics of the adsorption process. To the best of our knowledge, this is the first report on the synthesis, and application of polydopamine@Zeolitic Imidazolate-67 for removal of methylene blue from aqueous solution.

EXPERIMENTAL

Chemicals

All of the chemicals and reagents were used as received. $CoCl_2.6H_2O$ (analysis grade), 2-Methylimidazole (extra pure), MB (Art. No. 159270), Ethanol (96%), $KMnO_4$ (Art. No. 159270), and $K_2Cr_2O_7$ (Art. No. 109119), were purchased from Merck KGaA, Germany. Dopamine (DA, 3,4-dihydroxyphenethyl amine, extra pure) was purchased from Caspian Tamin pharmaceutical Company. Double distilled water was used as solvent in all of the experiments.

Instrumentation

Ultraviolet–visible (UV–Vis) spectra were recorded at room temperature (RT) on a Cary 5000 spectrophotometer. Energy-dispersive X-ray spectroscopy

(EDS) was performed using a Mira-3 XMu microanalyzer. Morphology of the PDA@ZIF-67 sample was studied by field emission scanning electron microscopy (FESEM, XL30 ESEM; Philips). BET measurements were performed on a BEL SORP mini II. A Milwaukee Mi806 pH-meter was used in all of the experiments.

Synthesis of ZIF-67

ZIF-67 nano-cubes were prepared in aqueous solution at room temperature (RT) according to a simple method [30]. Briefly, 450 mg of $Co(NO_3)_2.6H_2O$ was dissolved in 3 mL of double distilled water. Meanwhile 5.5 g of 2-methylimidazole (Hmim) was dissolved in 20 mL of double distilled water. The two solutions were mixed and stirred for 6 h at rt. The resulting purple precipitates were collected by centrifugation, washed with water and methanol consequently for 3 times, and finally vacuum-dried at 80 °C for 24 h.

Synthesis of PDA@ZIF-67

First, 30 mg of ZIF-67 was dispersed in a solution of 45 mg of dopamine in 30 mL of double distilled water in an ultrasonic bath. Afterwards, $KMnO_4$ (a full spatula, excess) was added and stirred for 6 h. Then the white precipitate was washed with water and ethanol for several times, and dried at 50 °C overnight. Potassium permanganate was used as a polymerization initiator and the main oxidant to convert dopamine to polydopamine. It should be noted that $K_2Cr_2O_7$ can be used as an initiator instead, as reported earlier [26].

Batch adsorption studies

To 100 mL of a 7.5 ppm solution of MB in double distilled water, 10 mg of PDA@ZIF-67 was added and the mixture was stirred by a magnetic stirrer at 150 rpm. The progress of adsorption was studied at different time intervals by sampling and filtration of the solution, followed by measuring the absorbance of the filtrate at 664 nm. Each measurement was repeated three times and the standard deviations were expressed as error bars.

pH of the solutions was adjusted to the desired value by using Britton–Robinson buffer, which is a universal pH buffer used for the pH range of 2 to 12 [26].

Recycling of the PDA@ZIF-67

Recovery and reuse of the PDA@ZIF-67 composite was performed as follows: after the first cycle, the PDA@ZIF-67 composite was separated by centrifugation at 3000 rpm, washed with double-distilled water (5 × 10 mL) and then with ethanol (3 × 10 mL). Finally, the precipitate was dried in an oven at 50 °C overnight. The recycled PDA@ZIF-67 was used consecutively for six cycles.

RESULTS AND DISCUSSION

Structural characterization of the adsorbent was carried out by FTIR and FESEM analyses. Figure 2a displays the FTIR spectrum of ZIF-67. Generally, the adsorption peaks in the range of 600-1500 cm^{-1} are attributed to the stretching and bending vibrations of imidazolate moiety [32]. The observed peak at 1578 cm^{-1} is attributed to the stretching vibration of C=N [33]. Also, the adsorption peak at 3135 cm^{-1} is related to the C-H bonds of the aromatic ring of 2-methylimidazole. Figure 2b shows the FTIR spectrum of PDA. The advent of a large and wide peak in the range of 3200-3600 cm^{-1}, well corroborates the presence of hydroxyl groups [34]. The adsorption peaks of amine functional groups are not seen in this spectrum due to the overlap of the intense hydroxyl peak [35]. The N-H bending vibrations, however, were observed at 1621 cm^{-1}. The C=C vibrations of the PDA structure were appeared at 1504 cm^{-1}. Figure 2c, on the other hand, represents the FTIR spectrum of PDA@ZIF-67. It can be seen that the anticipated peaks of the corresponding functional groups are present in the final product, without considerable changes in their position and intensity.

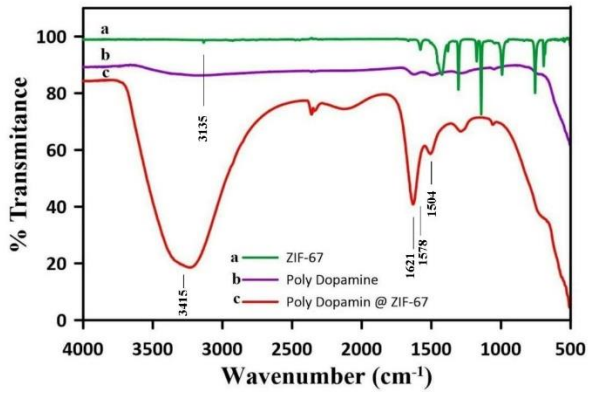


Fig. 2. FT-IR spectra of (a) ZIF-67, (b) polydopamine, and (c) PDA@ZIF-67 composite

Morphological study of the PDA@ZIF-67 was carried out by FESEM. Surface morphology of the PDA@ZIF-67 composite is shown in Figure 3. Clearly, the PDA@ZIF-67 composite is formed of many ultrafine nanoparticles in the range of 12-18 nm.

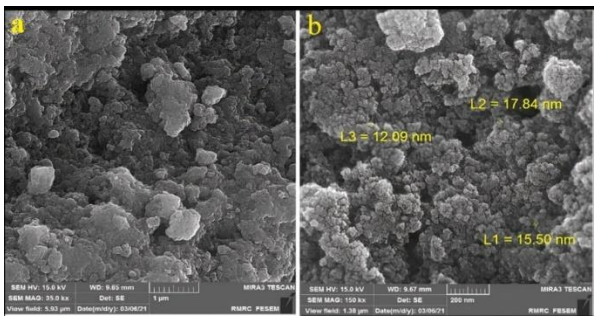


Fig. 3. FESEM images of the PDA@ZIF-67 composite.

EDS analysis was also used to evaluate the composition of the constituting elements of the PDA@ZIF-67. As shown in Figure 4, the corresponding K and L lines of each of the anticipated elements were present, with the C:Co ratio of 26.3:1.3%w/w.

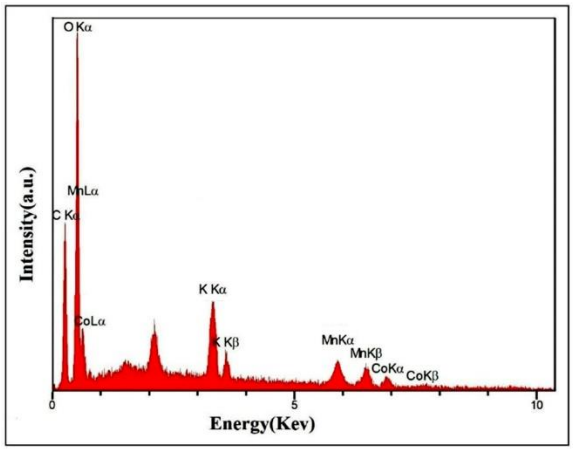


Fig. 4. EDS spectrum of the PDA@ZIF-67 composite.

BET analysis was used to study the physicochemical properties of PDA@ZIF-67 composite. The corresponding N_2 adsorption-desorption isotherm is shown in Figure 5a, where a type-IV isotherm is clearly visible with a distinct hysteresis loop in the P/P_0 range of 0.3-0.95. The specific surface area of the PDA@ZIF-67 was found to be 203.78 m^2g^{-1}. The corresponding BJH pore distribution curve (Figure 5b) was used to evaluate the pore structure of PDA@ZIF-67. As can be seen, two types of pores including micro- (<2 nm) and meso-pores (2-50 nm) were present with an average pore diameter of 4.179 nm.

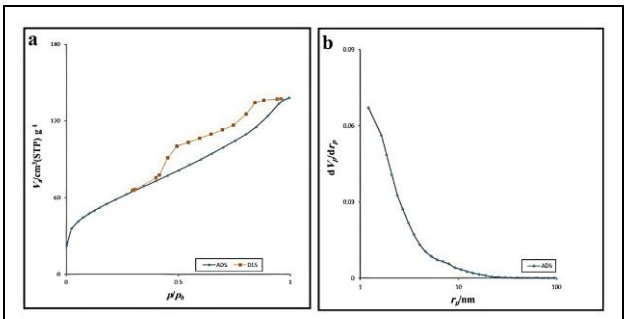


Fig. 5. (a) The N2 adsorption-desorption isotherm of PDA@ZIF-67, and (b) its corresponding BJH pore distribution curve

With the characterized PDA@ZIF-67 composite in hand, a systematic study was conducted to evaluate its adsorption capacity. First, we compared the adsorption of MB on polydopamine, Zeolitic Imidazolate-67, and PDA@ZIF-67 composite. To do so, a 2.5 ppm solution of MB in double distilled water was prepared. 10 mg of each adsorbent was added to 100 mL of the aforementioned solution. Up to 99% of MB removal was observed within 45 min by using the PDA@ZIF-67 synthesized in presence of potassium permanganate as a polymerization agent (to convert dopamine to polydopamine during the synthesis of PDA@ZIF-67).

Figure 6, shows the trend of MB adsorption in terms of C/C_0 vs. time for each of the adsorbents, where, C_0 is the initial concentration of dye solution, and C is its concentration at time t. As shown, the PDA@ZIF-67 can remove up to 99% of MB within 45 min at RT and neutral pH, when $KMnO_4$ was used as the polymerization initiator. In comparison, when $K_2Cr_2O_7$ was used as the polymerization initiator, PDA@ZIF-67 showed a lower adsorption capacity.

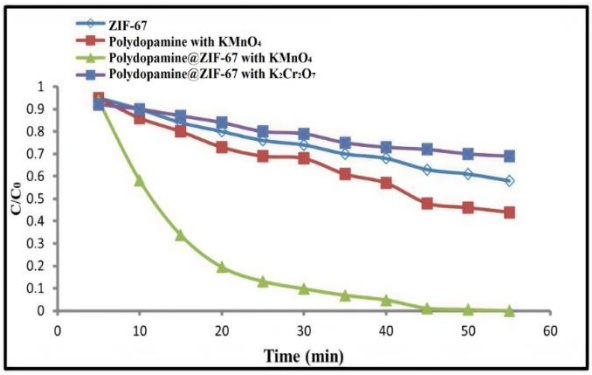


Fig. 6. The adsorption process of MB (2.5 ppm) over time in presence of 10 mg of each adsorbent at RT and neutral pH.

In order to optimize the polydopamine/ZIF-67 ratio, various proportions of each ingredient were tested. It was found that the optimal ratio of polydopamine to ZIF-67 was 45:30 (mg) as shown in Figure 7.

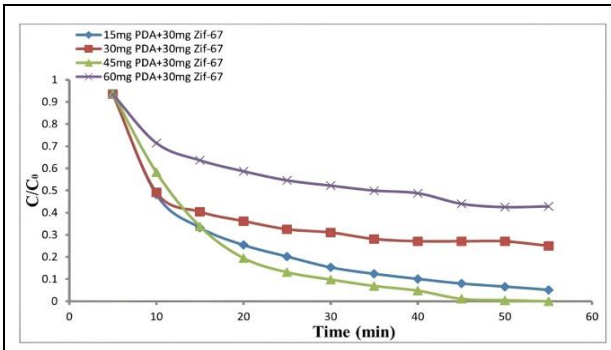


Fig. 7. The adsorption process of MB (2.5 ppm) over time in presence of 10 mg adsorbent synthesized with different polydopamine: ZIF-67 ratios at RT and neutral pH.

One of the key factors in the adsorption processes is the pH of solution. In this study, the Britton-Robinson buffer (Aka BBR or PEM) was used to adjust the pH in the range of 2-12, to study the effect of pH on the adsorption of MB [36]. Figure 8 illustrates the UV-Vis spectra of MB after 10 min in presence of 10 mg of the composite at different pH values (2, 4, 6, 8, 10, and 12). As shown, the maximum adsorption capacity was obtained at pH 2. As predicted, the adsorbent at the negative pH (pH<0) has a positive charge due to the protonation of the hydroxyl groups, so that the adsorption capacity at high acidic pH cannot be maximum. This observation is due to the fact that electrostatic interactions are not the dominant force in MB at pH 2**.** In fact, a high adsorption capacity for MB in the MB^+ form in acidic environment is obtained due to the π-π interactions, or formation of hydrogen bonds (Co--OH…NH) between the MB and PDA@ZIF-67 [37].

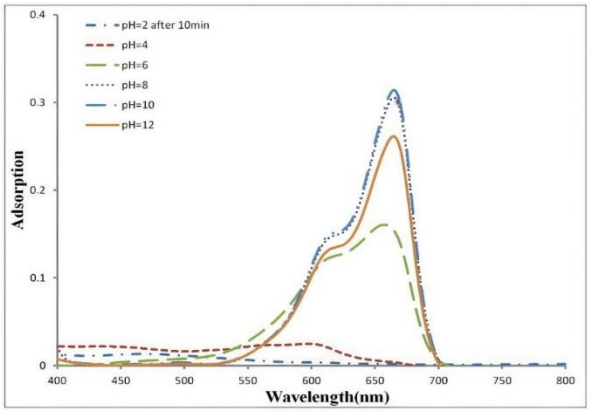


Fig. 8. UV-Vis spectra of MB (2.5 ppm) after treatment with 10 mg of PDA@ZIF-67 for 10 min at different pH.

Effect of the initial dye concentration on the adsorption process was also studied in presence of 10 mg of PDA@ZIF-67 to determine the optimal concentration of MB. All of the experiments were conducted at RT and pH 2 for 10 minutes. The corresponding UV-Vis spectra are shown in Figure 9, and the results are summarized in Table 1. According to the data of Table 1 and Figure 9, the optimal concentration of MB was determined to be 7.5 ppm.

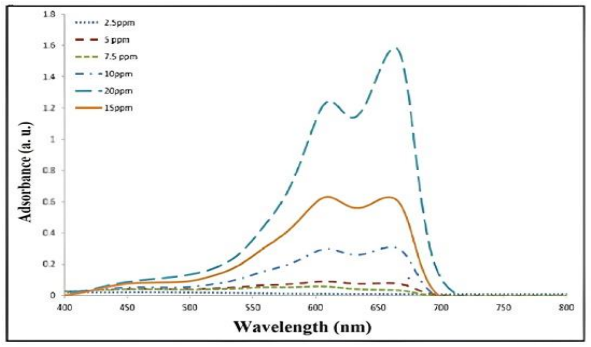


Fig. 9. Effect of the initial dye concentration on the UV-Vis spectra of MB dye solutions treated with 10 mg of PDA@ZIF-67 for 10 min at pH 2.

Table 1
The adsorption percentage of MB *vs.* concentration of dye after 10 min.[a] RT, pH 2, 10 mg of PDA@ZIF-67

MB concentration (ppm)	Adsorption efficiency (%)
2.5	94.61
5	93.13
7.5	89.64
10	72.91
15	65.84
20	47.76

To determine the optimal contact time, the adsorption process of MB (7.5 ppm) was studied at RT and pH 2 in presence of 10 mg of the adsorbent from 2 to 10 min. As shown, the optimal contact time for this process, was found to be 8 minutes with up to 89.50% removal of dye (Figure 10).

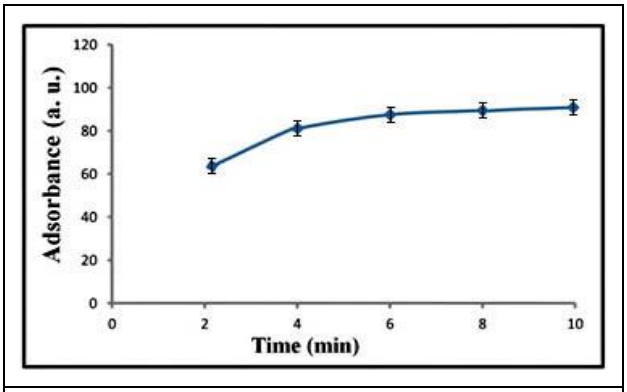


Fig. 10. Effect of contact time on the adsorption process of MB dye.

Eventually, the optimum temperature for the adsorption of MB was determined by studying the adsorption reaction at four different temperatures from 25 to 65°C. The obtained results are illustrated in Figure 11, where one can see that the adsorption of MB (100 mL, 7.5 ppm) after 8 min reached to the maximum (99.89%) at 65°C in presence of 10 mg of PDA@ZIF-67 at pH 2.

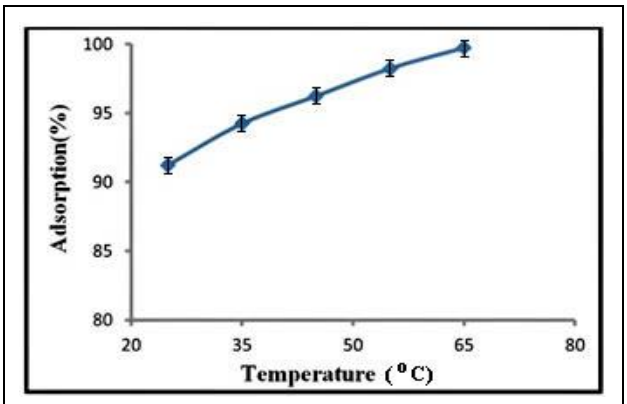


Fig. 11. Effect of temperature on the removal of MB (7.5 ppm, pH 2, 10 mg of PDA@ZIF-67).

Recyclability of the PDA@ZIF-67

The adsorption efficiency of an adsorbent after recycling is an important and crucial factor. As shown in Figure 12, a reasonable decrease in the removal capacity of PDA@ZIF-67 was observed. The recycled composite after the 6th run was able to remove up to 62.1% of MB.

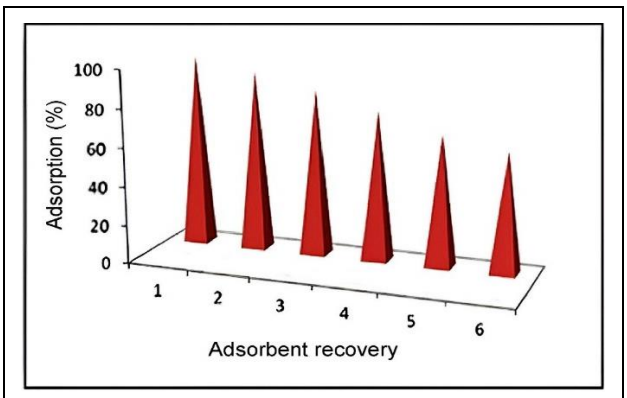


Fig. 12. Reuse of the PDA@ZIF-67 for six consecutive cycles.

Adsorption kinetics and isotherms

Study of the adsorption kinetics is very important to predict the adsorption mechanisms that control the pollutants removal, and the retention time of the adsorbed species. The adsorption kinetics can be explored by some kinetic models such as pseudo-first-order (PFO) [1], pseudo-second-order (PSO) [1], and intra-particle kinetics [38].

The pseudo-first-order equation is described as equation (1):

$$q_t=q_e(1-\exp^{-k_1 t}) \quad (1)$$

where, the unit of rate constant (k_1) is 1/min., and t is the adsorption time.

The Pseudo-second-order equation can be expressed as equation (2):

$$q_t=k_2 q_e^2 t/1+k_2 q_e^t \quad (2)$$

where, k_2 represents the rate constant of the pseudo-second-order equation (g/mg.min). The initial absorption velocity can be obtained using the values of k_2 and qe in the aforementioned equation.

The intramolecular diffusion model follows equation (3):

$$q_t=k_i t^{0/5}+C \quad (3)$$

where, C is related to the thickness of the boundary layer. The rate constant of intramolecular diffusion (k_i) is min/1. Table 2 shows the calculated parameters for the adsorption of MB by PDA @ ZIF-67.

Table 2
Kinetic parameters obtained from traditional models for MB adsorption (5 mg L^{-1})

Pseudo first-order			Pseudo second-order			Intra-particle diffusion		
q_e	K_1	R^2	q_e	K_2	R^2	K_{diff}	C	R^2
33.8 61	0.4 64	0.95 41	81 .3	0.0 18	0.99 97	9.85 78	48.2 58	0.96 61

The obtained q_e values from the pseudo-first-order kinetics model for MB adsorption is not consistent with the experimental data. The q-theoretic data values follow the pseudo-second-order model. According to the model, the intra-particle diffusion of the adsorption process creates a linear plot for q_t vs. $t^{0.5}$, implying that if the lines pass through the origin, the speed control step is shown with this model (Figure 13).

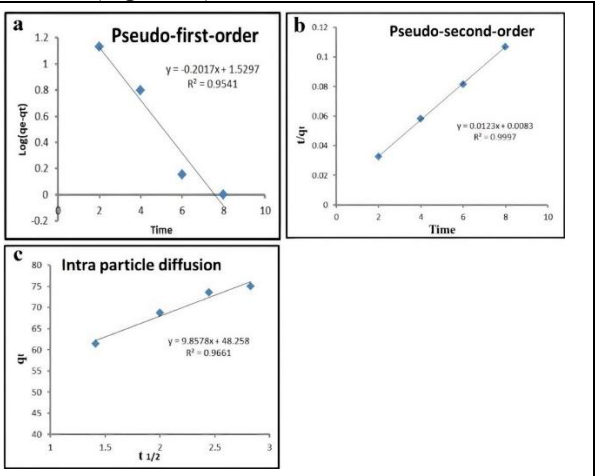


Fig. 13. (a-c) Pseudo-first order, pseudo-second order, and intra-particle model for dye adsorption on PDA@ZIF-67 utilizing linear equation.

The highest and lowest R^2 values belong to the pseudo-second-order and pseudo-first-order kinetics, respectively. Therefore, the adsorption of MB on PDA@ZIF-67 best fits to the pseudo- second order model. These results indicate that the rate-limiting phase of MB adsorption is the chemical adsorption phase of capacitance forces through the exchange or sharing of electrons between the adsorbent and the sorbent. To better understand the mechanism of the adsorption process, adsorption isotherms were used. Therefore, Langmuir, Freundlich, and Temkin isotherms were selected as the three most important isotherm models in this study.

The adsorption process was studied at a constant temperature. Adsorption isotherms are mathematical relationships that show the number of adsorbed molecules on the surface of the adsorbent. The adsorption properties of PDA@ZIF-67 toward MB at different concentrations of 2.5 to 20 mg/L was investigated.

A. Langmuir adsorption isotherm:

The Langmuir adsorption isotherm was developed by Irwin Langmuir in 1916 [22].

The Langmuir equation is as follows (equation (4)):

$$\frac{C_e}{q_e}=\frac{C_e}{q_{max}}+\frac{1}{q_{max}k_L} \quad (4)$$

Where, k_L denotes Langmuir constant (mg/L) and it means adsorption capacity at a pure level**.**

According to the Langmuir equation, the obtained values for K_L and q_{max} were 2.0833 L/mg, and 100 mg/g, respectively.

B. Freundlich adsorption isotherm

The Freundlich equation is as follows (equation (5)):

$$\ln q_e=\frac{1}{n}\ln C_e+\ln K_f \quad (5)$$

where, K_f is the Freundlich constant (mg/g), which represents the approximate index of Freundlich surface adsorption, and 1/n is the factor of surface adsorption strength during the adsorption process**.** The value of K_f based on the Freundlich equation was found to be 56.053 mg/g.

C. Temkin adsorption isotherm

The equation of Temkin described in the literature [25] is as follows (equation (6)):

$$q_e=\frac{RT}{b_T}\ln A_T+(\frac{RT}{b_T})\,ln\,C_e \quad (6)$$

where, q_e is the amount of solute adsorbed per unit weight of adsorbent (mg/g), Ce is the equilibrium concentration of MB (mg/L), R, A, T and b are the Temkin constants. According to the obtained parameters, the Langmuir, Freundlich and Temkin diagrams were drawn and interpreted. According to the diagrams (Figure 14) and Table 3, it can be concluded that the adsorbent follows the Langmuir adsorption isotherm (high values of R^2).

Table 3
The Langmuir, Freundlich and Temkin isotherms model constants and their correlation coefficients R^2 for the sorption of MB on PDA@ZIF-67.

Langmuir	Q_0 (mg/g)	101.3772
	b (L/mg)	0.2460
	R^2	0.9328
Freundlich	K_f (mg/g)	5112.109
	N (g/L)	4.8247
	R^2	0.9066
Temkin	K_t (mg/g)	0.8665
	B	13.3558
	R^2	0.8029

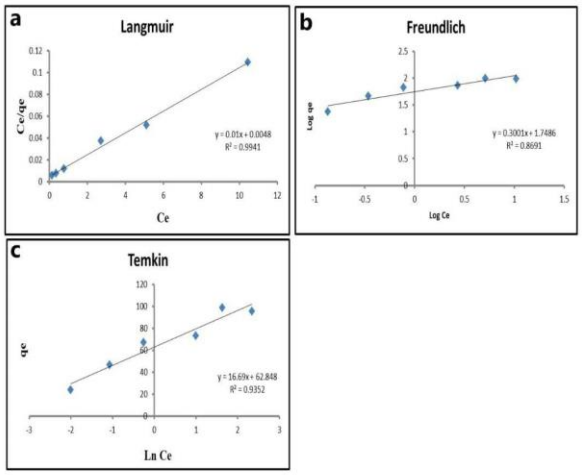


Fig. 14. (a-c) Langmuir, Freundlich, and Temkin isotherms for MB adsorption on PDA@ZIF-67 (Initial concentration of 7.5ppm, 65 °C).

Thermodynamics

The thermodynamic parameters were taken into account to characterize the adsorption operation on account of the 1 mole transfer of a solute from an aqueous solution on the solid-liquid interface. The empirical outcomes for adsorption of MB dye on PDA@ZIF-67 were applied at five various temperatures (298, 308, 318, 328, and 338 K) to evaluate the thermodynamics parameters such as Gibbs free energy (ΔG°, kJ/mol), entropy change (ΔS°, J/mol K), and enthalpy change (ΔH°, kJ/mol). The aforementioned parameters were calculated utilizing Van't Hoff equations (7, 8).

$$\ln K_d = \frac{\Delta S^\circ}{R} - \frac{\Delta H^\circ}{RT} \quad (7)$$

$$\Delta G^\circ = -RT\ lnK_d \quad (8)$$

Where, R, T, and K_L refer to the gas constant (8.314 J $mol^{-1}K^{-1}$), temperature (K), and Langmuir isotherm constant (L g^{-1}), respectively. The values of ΔG° were determined utilizing the Equation (9). Table 4 reveals the obtained thermodynamic parameters.

Table 4
Thermodynamic parameters of MB adsorption on PDA@ZIF-67

Temperature (K)	**Thermodynamic parameters**		
	ΔG°_a(KJ mol^{-1})	ΔH°_a(KJ mol^{-1})	ΔS°_a(J mol^{-1} K^{-1})
298.15	-11.0567	30.6512	140.132
308.15	-12.6887		
318.15	-13.8791		
328.15	-15.2529		
338.15	-16.7788		

ΔS°> 0 implies that the MB molecules adsorption is randomly increased at the solid/solution border of the adsorbent. Consequently, throughout the enhancement of MB adsorption on the adsorbent surface, the amount of MB in solution decreases, and the freedom of solvent particles and PDA@ZIF-67 interface accelerates. Therefore, there is a strong affinity between the PDA@ZIF-67 particles and MB molecules [39].

Additionally, the endothermic reaction can be corroborated with the improving adsorption capacity correlated with the increase in temperature. ΔG°<0 indicates that the process of adsorption is practical at RT and the increase of ΔG° values with growing temperature signifies that the adsorption process of MB on the PDA@ZIF-67 is more spontaneous at higher temperatures [36].

On the other hand, the ΔH° magnitude can provide an idea about the kind of adsorption. The evolved heat during physical adsorption is of the same magnitude order as the heats of condensation, for instance, 2.1 - 20.9 kJ mol^{-1}, whereas the heats of chemisorption generally fall between 80-200 kJ mol^{-1} [36]. In this research, the ΔH° value was 30.6512 kJ mol^{-1} and signifies that the adsorption of MB should be considered as chemisorption [40]. It has been observed that the adsorbent capacity was mainly a function of the initial concentration of MB, and qm generally increases with increasing initial concentration of MB [36]. In order to highlight the relative advantages of the present study with those reported previously, a comparison is made in Table 5.

Table 5
A comparison of the obtained results for PDA@ZIF-67 with other common adsorbents reported in the literature

Adsorbent	q(mg/g)	Experimental Conditions	Reference
PDA@ZIF-67	100	pH 2.0 Dye concentration: 7.5 mg/L Contact time: 8 min Temperature: 65°C Adsorbent dosage: 10 mg	Present work
MOF1	102.4	pH 7.0 Dye concentration: 10 mg/L Contact time: 2 h Temperature: 25°C	[41]
Laboratory paper	24	pH Neutral Dye concentration: 40 mg/L Contact time: 2 h Adsorbent dosage: 250 mg Temperature: 30°C	[14]
Fe3O4@MIL-100(Fe)	73.80	pH 9.0 Dye concentration: 60 mg/L Contact time: 120 min Adsorbent dosage: 100mg Temperature: 45°C	[42]
Magnetite@silica @pectin hybrid nanocomposite	85.18	pH 8.0 Dye concentration: 100 mg/L Contact time: 120 min Temperature: 25°C	[4]
Parthenium hysterphorus	39.7	pH 7.0 Dye concentration: 40 mg/L Contact time: 60 min	[24]
CuO loaded Activated Carbon 1	10.54	pH 6.0 Dye concentration: 50 mg/L Contact time: 4.5 min Adsorbent dosage: 1.1g/L Temperature: 25°C	[13]
Fly ash geopolymer powder	50.7	pH > 9 Dye concentration: 75 mg/L Contact time: 2 h Adsorbent dosage: 40mg Temperature: 25°C	[15]
Fe-BDC MOF	8.65	pH 9.0 Dye concentration: 5 mg/L Contact time: 24 h Adsorbent dosage: 2.5g/L Temperature: 323 K	[3]

A comparison of the data presented in Table 5 reveals that the adsorption capacity, q (the weight of pollutant adsorbed per gram of adsorbent (mg/g)), for the PDA@ZIF-67 is considerably higher than the other adsorbents. In comparison with MOF1 (entry 2), however, the advantage of PDA@ZIF-67 is reflected in the contact time (8 min *vs.* 2 h). These results can introduce PDA@ZIF-67 as an efficient adsorbent for removal of MB under mild conditions.

CONCLUSION

In the present work, a new hybrid crystalline porous material was synthesized by doping ZIF-67 with PDA. The resultant composite was used as an adsorbent to remove MB dye from aqueous solution. The PDA@ZIF-67 exhibited an excellent adsorption performance in removal of MB dye. The optimal conditions for the maximum adsorption efficiency were found to be dye concentration of 7.5 ppm, pH 2, 10 mg of PDA@ZIF-67 at 338 K. Under these optimized conditions, 99.89% of MB was removed within 8 min. The Langmuir isotherm was identified as the most favorable model to describe the adsorption process (Q_0= 101.37 mg/g). From the recyclability point of view, the recycled composite at the 6th run was able to remove up to 62.1% of MB. Based on the obtained results, it can be concluded that the PDA@ZIF-67 can be used as an effective adsorbent to remove MB from aqueous solutions. In future studies, one can aim to explore the scalability of polydopamine@Zeolitic Imidazolate-67 for industrial applications, investigate its modification, and assess its performance in the adsorption of a broader range of dye pollutants in aqueous solutions.

• Funding: Not applicable.
• Conflict of Interest: Not applicable.
• Ethical approval: Not applicable.
• Informed consent: Not applicable.

REFERENCES

[1] Mohammadinezhad A, Marandi GB, Farsadrooh M, Javadian H. Synthesis of poly (acrylamide-co-itaconic acid)/MWCNTs superabsorbent hydrogel nanocomposite by ultrasound-assisted technique: swelling behavior and Pb (II) adsorption capacity. Ultrasonics sonochemistry. 2018; 49:1-12.

[2] Choi Y, Lee J-H, Kim K, Mun H, Park N, Jeon J. Identification, quantification, and prioritization of new emerging pollutants in domestic and industrial effluents, Korea: Application of LC-HRMS based suspect and non-target screening. Journal of hazardous materials. 2021; 402:123706.

[3] Shindhal T, Rakholiya P, Varjani S, Pandey A, Ngo HH, Guo W, et al. A critical review on advances in the practices and perspectives for the treatment of dye industry wastewater. Bioengineered. 2021; 12(1):70-87.

[4] Dahiya D, Nigam PS. Waste management by biological approach employing natural substrates and microbial agents for the remediation of dyes' wastewater. Applied sciences. 2020; 10(8):2958.

[5] Wang S, Liu Y, Wang J. Peroxymonosulfate activation by Fe–Co–O-codoped graphite carbon nitride for degradation of sulfamethoxazole. Environmental Science & Technology. 2020; 54(16):10361-9.

[6] Vieira WT, de Farias MB, Spaolonzi MP, da Silva MGC, Vieira MGA. Removal of endocrine disruptors in waters by adsorption, membrane filtration and biodegradation. A review. Environmental Chemistry Letters. 2020; 18(4):1113-43.

[7] Wang K, Wei T, Li Y, He L, Lv Y, Chen L, et al. Flocculation-to-adsorption transition of novel salt-responsive polyelectrolyte for recycling of highly polluted saline textile effluents. Chemical Engineering Journal. 2021; 413:127410.

[8] Guillossou R, Le Roux J, Brosillon S, Mailler R, Vulliet E, Morlay C, et al. Benefits of ozonation before activated carbon adsorption for the removal of organic micropollutants from wastewater effluents. Chemosphere. 2020; 245:125530.

[9] Sohrabnezhad S, Pourahmad A, Karimi MF. Magnetite-metal organic framework core@ shell for degradation of ampicillin antibiotic in aqueous solution. Journal of Solid-State Chemistry. 2020; 288:121420.

[10] Piai L, Blokland M, van der Wal A, Langenhoff A. Biodegradation and adsorption of micropollutants by biological activated carbon from a drinking water production plant. Journal of hazardous materials. 2020; 388:122028.

[11] Albatrni H, Qiblawey H, El-Naas MH. Comparative study between adsorption and membrane technologies for the removal of mercury. Separation and purification technology. 2021; 257:117833.

[12] Aleem M, Cao J, Li C, Rashid H, Wu Y, Nawaz MI, et al. Coagulation-and adsorption-based environmental impact assessment and textile effluent treatment. Water, Air, & Soil Pollution. 2020; 231:1-8.

[13] Kuśmierek K, Świątkowski A, Skrzypczyńska K, Dąbek L. Adsorptive and electrochemical properties of carbon nanotubes, activated carbon, and graphene oxide with relatively similar specific surface area. Materials. 2021;14(3):496.

[14] Hızal J, Yılmazoğlu M. Montmorillonite clay composite for heavy metal removal from water. Green Adsorbents to Remove Metals, Dyes and Boron from Polluted Water. 2021:93-112.

[15] Chen M, Shen Y, Xu L, Xiang G, Ni Z. Synthesis of a super-absorbent nanocomposite hydrogel based on vinyl hybrid silica nanospheres and its properties. RSC advances. 2020;10(67):41022-31.

[16] Thabet RH, Tony MA, El Sherbiny SA, Ali I, Fouad MK, editors. Catalytic oxidation over nanostructured heterogeneous process as an effective tool for environmental remediation. IOP conference series: materials science and engineering; 2020: IOP Publishing.

[17] Chai J-B, Au P-I, Mubarak NM, Khalid M, Ng WP-Q, Jagadish P, et al. Adsorption of heavy metal from industrial wastewater onto low-cost Malaysian kaolin clay–based adsorbent. Environmental Science and Pollution Research. 2020;27(12):13949-62.

[18] Atun G, Ortaboy S, Tüzün E, Türker Acar E. A comparison of anionic and cationic dye removal efficiency of industrial bauxite waste red-mud. Journal of Dispersion Science and Technology. 2023;44(1):144-56.

[19] Vučković N, Nikodijević M, Đorđević D. The study of direct dye sorption on flax fibers during dyeing. Chemical Industry and Chemical Engineering Quarterly. 2021;27(3):255-63.

[20] Sahu S, Pahi S, Tripathy S, Singh SK, Behera A, Sahu UK, et al. Adsorption of methylene blue on chemically modified lychee seed biochar: Dynamic, equilibrium, and thermodynamic study. Journal of Molecular Liquids. 2020; 315:113743.

[21] Lee HA, Park E, Lee H. Polydopamine and its derivative surface chemistry in material science: a focused review for studies at KAIST. Advanced Materials. 2020;32(35):1907505.

[22] Huang L, Miao J, Shuai Q. Carboxyl-functionalized magnetic porous organic polymers as efficient adsorbent for wastewater remediation. Journal of the Taiwan Institute of Chemical Engineers. 2020; 109:97-102.

[23] Zhang M, Zhang Z, Peng Y, Feng L, Li X, Zhao C, et al. Novel cationic polymer modified magnetic chitosan beads for efficient adsorption of heavy metals and dyes over a wide pH range. International journal of biological macromolecules. 2020; 156:289-301.

[24] Qiu M, He C. Efficient removal of heavy metal ions by forward osmosis membrane with a polydopamine modified zeolitic imidazolate framework incorporated selective layer. Journal of hazardous materials. 2019; 367:339-47.

[25] Lu Y, Zhan W, He Y, Wang Y, Kong X, Kuang Q, et al. MOF-templated synthesis of porous Co3O4 concave nanocubes with high specific surface area and their gas sensing properties. ACS applied materials & interfaces. 2014;6(6):4186-95.
[26] Jamdar M, Monsef R, Ganduh SH, Dawi EA, Jasim LS, Salavati-Niasari M. Unraveling the potential of sonochemically achieved DyMnO3/Dy2O3 nanocomposites as highly efficient visible-light-driven photocatalysts in decolorization of organic contamination. Ecotoxicology and Environmental Safety. 2024; 269:115801.
[27] Jafarinejad A, Salavati-Niasari M, Monsef R, Bashiri H. Flower-shaped magnetically recyclable ZnS/ZnIn2S4/Fe2O3 nanocomposites towards decolorization of colored pollutants. International Journal of Hydrogen Energy. 2023;48(9):3440-55.
[28] Panahi A, Monsef R, Hussein SA, Hammood SA, Al-Azzawi WK, Raffik DE, et al. Multidisciplinary methods for synthesis of visible-light-driven TmVO4 nanostructure photocatalyst with enhanced photocatalytic activity towards removal of toxic contaminates. International Journal of Hydrogen Energy. 2023;48(85):33155-65.
[29] Hosseini M, Ghanbari M, Dawi EA, Mahdi MA, Ganduh SH, Jasim LS, et al. Investigations of nickel silicate for degradation of water-soluble organic pollutants. International Journal of Hydrogen Energy. 2024;61:307-15.
[30] Bioumy SA, Ahmed RA, Fekry AM. Electrochemical corrosion behavior of graphene oxide/chitosan/silver nanoparticle composite coating on stainless steel utensils in aqueous media. Journal of Bio-and Tribo-Corrosion. 2020;6(3):78.
[31] Khan A, Ali M, Ilyas A, Naik P, Vankelecom IF, Gilani MA, et al. ZIF-67 filled PDMS mixed matrix membranes for recovery of ethanol via pervaporation. Separation and Purification Technology. 2018; 206:50-8.
[32] Li Y, Jin Z, Zhao T. Performance of ZIF-67–Derived fold polyhedrons for enhanced photocatalytic hydrogen evolution. Chemical Engineering Journal. 2020; 382:123051.
[33] Ho C-C, Ding S-J. The pH-controlled nanoparticles size of polydopamine for anti-cancer drug delivery. Journal of Materials Science: Materials in Medicine. 2013; 24:2381-90.
[34] Batul R, Bhave M, J. Mahon P, Yu A. Polydopamine nanosphere with in-situ loaded gentamicin and its antimicrobial activity. Molecules. 2020;25(9):2090.
[35] Utsev J, Iwar R, Ifyalem K. Adsorption of methylene blue from aqueous solution onto delonix regia pod activated carbon: batch equilibrium isotherm, kinetic and thermodynamic studies. Agric waste. 2020;4(5):18.
[36] Yi FY, Li JP, Wu D, Sun ZM. A series of multifunctional metal–organic frameworks showing excellent luminescent sensing, sensitization, and adsorbent abilities. Chemistry–A European Journal. 2015;21(32):11475-82.
[37] Hooshyar SP, Panahi HA, Moniri E, Farsadrooh M. Tailoring a new hyperbranched PEGylated dendrimer nano-polymer as a super-adsorbent for magnetic solid-phase extraction and determination of letrozole in biological and pharmaceutical samples. Journal of Molecular Liquids. 2021; 338:116772.
[38] Li M, Sun P, Wu Q, Liu D, Zhou L. Core–shell magnetic metal–organic framework molecularly imprinted nanospheres for specific adsorption of tetrabromobisphenol A from water. Environmental Science: Nano. 2018;5(11):2651-62.
[39] Durairaj A, Sakthivel T, Ramanathan S, Obadiah A, Vasanthkumar S. Conversion of laboratory paper waste into useful activated carbon: a potential supercapacitor material and a good adsorbent for organic pollutant and heavy metals. Cellulose. 2019; 26:3313-24.
[40] Yang Q, Zhao Q, Ren S, Lu Q, Guo X, Chen Z. Fabrication of core-shell Fe3O4@ MIL-100 (Fe) magnetic microspheres for the removal of Cr (VI) in aqueous solution. Journal of Solid-State Chemistry. 2016; 244:25-30.
[41] Attallah OA, Al-Ghobashy MA, Nebsen M, Salem MY. Removal of cationic and anionic dyes from aqueous solution with magnetite/pectin and magnetite/silica/pectin hybrid nanocomposites: kinetic, isotherm and mechanism analysis. RSC advances. 2016;6(14):11461-80.
[42] Lata H, Garg V, Gupta R. Removal of a basic dye from aqueous solution by adsorption using Parthenium hysterophorus: an agricultural waste. Dyes and pigments. 2007;74(3):653-8.